Flexural Strengthening of Steel Bridges with High Modulus CFRP Strips

David Schnerch[1] and Sami Rizkalla, F.ASCE[2]

CE Database Subject Headings: Adhesive Bonding, Bridges, Composite Beams, Composite Materials, Fiber Reinforced Polymers, Flexural Strength, Prestressing, Rehabilitation, Steel Structures (9 max)

Abstract: Acceptance of carbon fiber reinforced polymer (CFRP) materials for strengthening concrete structures, together with the recent availability of higher modulus CFRP strips, has resulted in the possibility to also strengthen steel structures. Steel bridge girders and building frames may require strengthening due to corrosion induced cross-section losses or changes in use. An experimental study investigating the feasibility of different strengthening approaches was conducted. Large-scale steel-concrete composite beams, typical of bridge structures, were used to consider the effect of CFRP modulus, prestressing of the CFRP strips, and splicing finite lengths of CFRP strips. All of the techniques examined were effective in utilizing the full capacity of the CFRP material, and increasing the elastic stiffness and ultimate strength of the beams. Results of the experimental program were compared to an analytical model that requires only the beam geometry and the constitutive properties of the CFRP, steel and concrete. This model was used to investigate the importance of several key parameters. Finally, an approach for design is proposed that considers the bilinear behavior of a typical strengthened beam to the elastic-plastic behavior of the same beam before strengthening.

---

[1] Engineering Associate, Wiss, Janney, Elstner Associates, Inc., 245 First Street, Suite 1200, Cambridge, MA 02142-1292. E-mail: dschnerch@wje.com

[2] Distinguished Professor of Civil Engineering and Construction, and Director of the Constructed Facilities Laboratory, Department of Civil, Construction, and Environmental Engineering, North Carolina State University, Raleigh, NC 27695-7908

Introduction/ Background

Early applications of bonded fiber reinforced polymer (FRP) materials for repair and strengthening of metallic structures have been for thin-walled steel or aluminum structures. Aerospace and naval industries have made use of carbon fiber reinforced polymer (CFRP) materials for repair of fatigue damage (Armstrong 1983, Allan *et al.* 1988, and Aglan *et al*. 2001). The offshore oil and gas industry has also made use of CFRP materials for increases in blast protection (Galbraith and Barnes 1995). Particularly noteworthy is the extreme environmental conditions that these structures may be subjected to, involving large changes in temperature or exposure to saline environments. CFRP strengthening is attractive for steel bridges and structures since it avoids field welding, particularly overhead welding, that strengthening with steel requires.

For investigations considering civil engineering structures, there have been fewer investigations of strengthening wide-flanged beams strengthened with FRP materials than either beams acting compositely with a concrete deck or beams that have a tension flange defect, such as a notch. As Liu *et al*. (2001) correctly notes, strengthening of a wide-flange beam on the tension side alone results in a strain profile that shifts the neutral axis towards the CFRP material. As such, the CFRP material is not effectively utilized since the lever arm between the neutral axis and the CFRP material is small, and gets smaller with continued yielding of the section of the compression side. Furthermore, the CFRP material may never reach its rupture strain until after much of the remainder of the section is in compression and stability of the compression flange becomes the dominant factor in controlling the behavior.

CFRP strengthening of intact wide flange beams was investigated by Edberg *et al*. (1996), where several configurations were developed to increase the distance between the bottom flange and the centroid of the CFRP strip, including the use of a thick aluminum honeycomb layer inserted between the beam soffit and the strengthening material. Colombi and Poggi (2006) tested wide flange beams with one or two layers of CFRP strips. For the specimens with one ply of CFRP strips, the reported stiffness increase of the strengthened beam was minimal. The stiffness increase for two layers of CFRP strips was found to be 13.8 percent. Strengthening of steel structures with standard modulus CFRP materials has typically shown small stiffness increases.

Steel-concrete composite beams are a common structural system due to their material efficiency by using the steel wide-flange section in tension and the concrete deck in compression, while also providing lateral support to the steel beam. Previous research has shown the effectiveness of strengthening steel-concrete composite beams with CFRP materials in improving the ultimate strength of steel-concrete composite girders, but with little increase of the elastic stiffness (Sen *et al*. 2001 and Tavakkolizadeh and Saadatmanesh 2003).

In the United Kingdom, numerous historic cast iron and steel bridges have been successfully strengthened using CFRP materials (Luke 2001, Hollaway and Cadei 2002). The United States has been slower to adopt the technique for steel structures, but at least two bridges have been strengthened with bonded, standard modulus, CFRP strips. Bridge 1-704 over Christina Creek in Delaware was selected as a demonstration project for strengthening with CFRP strips (Miller *et al*. 2001). The bridge has high traffic loads, with 6000 trucks crossing the bridge daily. Strengthening was completed using 5.3 mm thick strips, resulting in a stiffness increase of 12 percent, based on vehicle load tests. Using the method of transformed sections, a strain decrease of 10 percent was predicted, although no particular amount of strengthening was required and the focus of the project was directed towards providing long-term performance and durability data. Three spans of a bridge in Iowa were also strengthened by bonding CFRP strips in the positive moment regions (Phares *et al*. 2003). Analysis showed that the stiffness of the bridge girders could be modestly increased by 1.2 percent per ply of CFRP strips (Lee *et al*. 2005). Different strengthening configurations were applied with the intent of examining the long-term durability.

Objective

The objective of this paper is to examine the behavior of large-scale steel-concrete composite beams that are typical of those used for bridge structures when strengthened with high modulus CFRP materials. Testing of the steel-concrete composite beams allowed comparison with the proposed analytical model. The paper also examines several details that are applicable to strengthening of steel bridges in the field. The potential of splicing finite lengths of CFRP strips was examined, since the lengths required for long span structures may be difficult to transport. A simple fixture was also made to machine a 20-degree reverse taper at the ends of the CFRP to

examine the practicality of minimizing critical bond stresses by controlling the geometry of the CFRP and adhesive bondline. The research also examined the concept of prestressing using a simple, specially designed fixture that allowed stressing of the CFRP strips during their application and curing.

Material Properties

High Modulus CFRP Material

Two types of high modulus pitch-based carbon fibers were used in the experimental program. Pitch-based carbon fiber utilizes petroleum pitch fiber as its precursor, unlike the more common PAN based carbon fiber that utilizes polyacrylonitrile. A CFRP strip using an intermediate modulus carbon fiber was used to strengthen one of the beams for comparison with the two beams that were strengthened using CFRP strips using the high modulus fiber. These two types of carbon fiber were pultruded into one of two types of unidirectional strips. The properties for the two types of strips, as determined by an external laboratory are listed in Table 1. The intermediate modulus fiber was used for the DC-I strips and the high modulus fiber was used for the THM 450 strips.

Concrete and Steel Properties

Mechanical properties for the concrete were determined at 28 days after casting and at the time of testing. Statistical analysis revealed that there was no significant difference in the concrete strength at 28 days compared to the concrete strength at the time of testing. In addition to the concrete strength, the full stress-strain behavior of the concrete was determined for later use with the analytical model. Sheet type steel coupons were also taken from the web and flange of pieces that were cut from the same steel as the beam specimens. Four coupons were taken from the flange and three coupons were taken from the web for both types of steel used. Finally, tension testing of the reinforcing steel was also completed. The yield strength of the reinforcing bars was determined using the 0.2 percent offset relationship. The material properties for each of the beams are listed in Table 2.

Experimental Program

Fabrication

Three large-scale steel-concrete composite beam specimens were fabricated using grade A992/A572-50 steel

W310 x 45 sections that were 6550 mm in length. Staggered shear studs were welded at a spacing of 152 mm along the length of the compression flange to ensure full composite action. The concrete deck was reinforced with grade 60 steel reinforcing bars that were 12.7 mm in diameter. Deck dimensions and spacing of the longitudinal concrete reinforcement are as shown in Figure 1. Transverse reinforcement was provided at a constant spacing of 152 mm. End blocks were cast with the deck, fully encasing the steel beam at the ends, to provide lateral stability and to eliminate the possibility of web crippling at the supports during loading.

Different strengthening configurations were used for each of the three specimens, with the designation of each specimen based on three different parameters. The first parameter indicates the modulus of the fiber used for the strengthening, whether high-modulus (HM) or intermediate modulus (IM). The second parameter indicates the CFRP reinforcement ratio of the applied strengthening, defined as the ratio of the cross-sectional area of the CFRP strip, taking into account the fiber volume fraction of the strips used, to the cross-sectional area of the steel section. The final parameter indicates whether the strengthening was achieved by adhesively bonding (AB) without stressing the CFRP strips or by prestressing the CFRP strips before bonding (PS).

For steel-concrete composite beam IM-4.5-AB, two DC-I type strips were used with a length of 4000 mm and cross section dimensions of 73 mm by 3.2 mm. The effectiveness of a spliced connection was investigated by bonding additional 1000 mm long strips on either side of the main longitudinal strips and covering the joint with additional 400 mm long pieces of the same type of strip. As a precaution against debonding, the strips were wrapped transversely around the flange by wet lay-up of 330 mm wide unidirectional carbon fiber sheets at the splice locations and at the ends of the 1000 mm long pieces. The test of beam HM-3.8-PS used one prestressed THM-450 strip that was 98 mm wide with a nominal thickness of 2.9 mm. For beam HM-7.6-AB, two THM-450 strips each with a width of 77 mm and a nominal thickness of 4.0 mm were used. Figure 2 shows the lengths of the longitudinal reinforcement and the locations of the transverse wraps for each of the three beams.

Specimens IM-4.5-AB and HM-3.8-PS were cast from the same concrete batch, while specimen HM-7.6-AB was

cast separately. Immediately following finishing of the concrete surface, the specimens were covered using a plastic sheet. The surface of the concrete was kept wet for the seven days following casting, after which time the specimens were released from the formwork and allowed to air cure. To prepare the beams for strengthening, each beam was sandblasted until a white metal surface was achieved along the underside of the tension flange and where any transverse wrapping using CFRP sheets was to be applied. Sandblasting and the longitudinal strengthening were conducted in a single day to minimize oxidation of the freshly sandblasted steel surface. Following sandblasting, dust was removed from the surface of the beam by blowing with compressed air. Further cleaning was performed by brushing the surface with acetone. Acetone was applied in excess so that it dripped from the beam, so as to remove any dissolved particles rather than merely redistributing them once the acetone had evaporated from the surface. Further details of the surface preparation are provided in Schnerch (2005).

The intermediate modulus DC-I type of CFRP strip was manufactured without a peel ply. To ensure adequate adhesion of this strip, the surface was lightly hand sanded with 120 grit sandpaper. The strips were then cleaned with methanol. The high modulus THM 450 strips were manufactured with a glass-fiber peel-ply and a rough-textured surface. This peel-ply protected the surface of the strip, but could be easily removed immediately prior to bonding with no surface preparation necessary after its removal. For both types of strips, a 20-degree bevel was machined with a simple fixture and a belt-type sander, as shown in Figure 3. This detail provided a sharp edge to the CFRP strip. The strip was applied to the beam, such that the adhesive bondline thickness was locally increased towards the end of the strip, while the cross-sectional area of the strip was decreased correspondingly, reducing the stress concentration that typically occurs at the ends of the strips. All CFRP strips used in the study were bonded using Spabond 345 epoxy resin, manufactured by SP Systems. The freshly mixed epoxy was applied directly to the surface of the CFRP material. To ensure a uniform bond-line, the epoxy was spread over the surface with a V-notch trowel with a notch depth of 5 mm. Additional epoxy was placed at the ends of the strip to ensure an adequate spew fillet would be achieved, also minimizing the stress concentration at the ends of the strip (Clarke, 1996). Immediately after the strips were applied, and before the pot life of the epoxy had expired, the CFRP strips were clamped in place by means of self-reacting wooden clamps.

For the beam using the prestressed strips, several additional steps were completed in the installation process. Steel tabs were fabricated that would be used to apply the prestressing force. Once the surface of the tabs was prepared by sandblasting, the tabs were bonded to the CFRP strip at the ends and allowed to cure. Prior to sandblasting the beam, two holes were drilled into the bottom flange of the steel beam to mount the tab used at the fixed-end. Two additional holes were drilled at the other end of the beam to mount the fixed pieces of the fixture used to apply the prestressing force, as shown in Figure 4. Adhesive was applied to the entire CFRP strip on the side that would be in contact with the beam. The steel tab at the fixed end was first bolted to the steel beam, and then the tab at the other end of the CFRP strip was inserted into the fixture to apply the prestressing force. The prestressing force was applied by means of tightening fine-threaded bolts that were positioned on each side of the fixture, as shown in Figure 5. These threaded bolts were located at the same level as the CFRP strip to avoid eccentric loading. Prestressing force was monitored by the use of strain gauges that were bonded to the CFRP strips at midspan until the design prestressing strain of 0.06 percent was achieved. Finally, the strips were clamped to the surface of the steel beam using the same self reacting wooden frames. The prestressing fixture was designed to be demountable, so that after the adhesive cured, the entire fixture except for the tabs may be removed and reused for other beams.

Testing Configuration and Instrumentation

The strengthened steel-concrete composite beam specimens, spanning 6400 mm, were tested under four-point loading, as shown in Figure 6. The constant moment region was 1000 mm, with two equal shear spans of 2700 mm. Neoprene pads were used at the supports and under the load points to allow for rotation. Loading was applied across the full width of the concrete slab by the use of 150 mm deep steel HSS sections that were placed between the spreader beam and the neoprene pads on the top of the beam. All tests in this series were performed under displacement control. Each of the steel-concrete composite beams was loaded three times. The first loading cycle was completed before strengthening to induce a strain of 0.12 percent in the tension flange, or approximately 60 percent of the yield stress. After strengthening, the second loading cycle was applied to induce the same stress as the first loading cycle. In the third cycle, the beam was loaded to failure.

All of the beams were instrumented with wire potentiometers to monitor deflection at both quarter points, at both load points, and at midspan. Additional potentiometers were used to measure the settlement of the supports. Two types of strain gauges were used for the tests. Electrical strain gauges were used at various locations on the CFRP strips and on the steel surface to measure the localized strain over a gauge length of 6 mm. These gauges were positioned at both quarter points, at midspan, and under the load points on the CFRP strips. Additional strain gauges were used for beam IM-4.5-AB to determine the effectiveness of the spliced connection of the CFRP strips. Strain gauge type displacement transducers were also used to measure the longitudinal strain of the top surface of the concrete deck and the bottom surface of the tension flange over a longer 200 mm gauge length.

Test Results and Discussion

Beam IM-4.5-AB

The first loading of the beam after strengthening showed the effectiveness of the intermediate modulus CFRP strips to increase the flexural stiffness by 10 percent. No degradation of the stiffness was apparent for the second loading, until after yielding of the steel, shown in Figure 7. The ultimate load, recorded immediately before rupture of the CFRP strips, was 418 kN. The measured maximum CFRP strip strain, occurring at midspan, was 0.450 percent. This is slightly less than the ultimate strain of the strips subjected to pure tension conditions, determined by the manufacturer to be 0.508 percent. Figure 7 shows the strain profile at three different curvatures and immediately before failure. The profiles indicate that the strain profile was essentially linear until yielding of the steel. Following yielding, at about 0.20 percent, shear lag was apparent whereby the CFRP had a lower strain than expected due to the lower stiffness of the adhesive compared to the steel and CFRP materials. To evaluate the effectiveness of the splice, the moment-curvature behavior was determined at midspan and at the splice locations. The moment curvature behavior near the splice location exactly followed the behavior at midspan, indicating the splice was as effective as the continuous strip at midspan, Schnerch (2005).

Rupture of the strips occurred within the constant moment region. Due to the sudden release of energy from the rupture, the strips debonded away from the rupture area. The debonding surface was partially between the

adhesive and the strip and partially within the strip itself, leaving a thin layer of FRP bonded to the beam in some locations. No debonding or other distress was observed from the location of the splice to the ends of the beam, where the splice was wrapped transversely with sheets around the top of the tension flange. Continued loading after rupture of the strips resulted in concrete crushing near one of the load points. The concrete crushing load represents the ultimate load of an unstrengthened beam, since after rupture of the strips most of the strengthening material was no longer effective. As such, the ultimate load increase for this beam was 18 percent.

Beam HM-3.8-PS

Steel-concrete composite beam HM-3.8-PS was strengthened with prestressed, high modulus CFRP strips in order to use the CFRP material more economically by increasing the beam stiffness, without enhancing its ultimate strength. The displacement of the beam, measured before loading, indicated a midspan camber of 1.9 mm after application of the prestressing. Once the epoxy had cured, the beam was again loaded to the same tension flange strain as in the first cycle of loading of the unstrengthened beam. Considering only the slope of the elastic responses before and after strengthening, a stiffness increase of 13 percent was achieved. However, considering the effect of the camber in the service range, an effective stiffness increase of at least 31 percent was achieved.

For the second loading to ultimate, shown in Figure 8, no degradation of the stiffness compared to the first loading was observed. Rupture of the CFRP strips occurred at a strain of 0.33 percent. The rupture strain of the CFRP strips can be attributed to the two components of loading. The first component of the strain was due to the flexural loading (0.27 percent) and the second was due to the initial prestressing (0.06 percent). Similar to the beam strengthened with the intermediate modulus sheets, rupture occurred at a strain slightly below the failure strain under conditions of pure tension reported by the manufacturer. Strain measurements also indicated that there were negligible short-term losses in the applied prestressing force. Strain profiles were determined at midspan. Until rupture, the strains were essentially linear at all stages of loading, also shown in Figure 8. Rupture of the strips occurred within the constant moment region. The energy released at rupture resulted in delamination

within the CFRP strip itself. Continued loading past rupture of the strips resulted in concrete crushing at one of the load points. As intended, the load at rupture was lower than the load at concrete crushing.

Beam HM-7.6-AB

This beam used twice the amount of the high modulus CFRP material compared to the previously tested prestressed beam. The first two cycles of loading, first of the unstrengthened beam, then of the strengthened beam, resulted in a stiffness increase of 34 percent in the elastic range, with no degradation of the stiffness upon reloading. A significant ultimate strength increase was observed just before rupture of the strips at 0.33 percent, as shown in Figure 9. Continued loading of the beam past rupture resulted in failure of the beam due to concrete crushing. Strain profiles shown in Figure 9 were essentially linear until well after yielding.

The sudden nature of rupture resulted in most of the strip becoming detached from the beam, as shown in Figure 10. The failure surface was mixed between the interface between the strip and the adhesive and within the strip itself. Considering that the load at concrete crushing may be taken as the ultimate strength of an unstrengthened beam, a 46 percent increase in the ultimate strength was achieved due to the strengthening.

Discussion

For the beams strengthened using the CFRP plates that were not prestressed, increases in ultimate strength were possible. Similar to the findings of Sen *et al*. (2001) and Tavakkolizadeh and Saadatmanesh (2003), most of the strength increase occurred in the region between first yielding of the section and rupture of the CFRP. Unlike the work of these authors, however, significant service level stiffness increases were also possible due to the use of the higher modulus of the CFRP material used in this study. Furthermore, significant service load increases were possible in using the high modulus CFRP strips, as shown in Table 3. Taking the load of the unstrengthened beam to induce 60 percent of the yield stress in the tension flange of the beam and comparing with the load of the strengthened beam at the same stress level in the tension flange, load increases of 10 percent, 31 percent and 36 percent were achieved for beams IM-4.5-AB, HM-3.8-PS and HM-7.6-AB, respectively.

A comparison of the beam properties at FRP rupture and at concrete crushing is provided in Table 4. Two of the strengthened beams resulted in an ultimate strength increase. The beam using the prestressed CFRP strips was designed so that the CFRP strips would rupture below the ultimate strength of the beam to preserve its original ductility. All of the beams failed at a deflection greater than the serviceability limit deformation of L/800 or 8 mm and the serviceability limit load capacity. The ultimate load capacity also exceeded the serviceability limit load capacity. None of the beams failed by debonding of the CFRP strips, indicating that the bonding and surface preparation technique was satisfactory to prevent this undesirable failure mode. The failure of the strips by rupturing is also associated with the use of the higher modulus strips. Rupture is a more likely failure mode due to the lower rupture strain of these strips. Also, since thinner strips may be used for a given strengthening level, these thinner strips will subject the adhesive to lower normal or peeling stresses at the ends.

The strain profile for beam IM-4.5-AB with the intermediate modulus CFRP strips showed a small amount of shear lag, in that the longitudinal strains in the CFRP were smaller than what would be expected from extrapolation of the strain profile over the remainder of the cross section. El Damatty *et al*. (2003) showed analytically that for GFRP strips with a lower modulus than the steel there would be significant shear lag. After yielding of the steel, the GFRP material would have a higher stiffness, and the lag would reverse. Experimentally, Sen *et al*. (2001) have also observed this effect for most of the steel-concrete composite beams that were strengthened with CFRP strips, where the strain profiles were essentially linear until after steel yielding. Dawood (2005) has shown, through more extensive testing of similar beams, that shear lag is negligible for the epoxy studied in conjunction with the high modulus CFRP strips.

Analytical Model

Design Principles and Assumptions

A moment-curvature procedure has previously been developed for prestressed concrete beams by Mattock (1979). This approach has been found suitable for predicting the flexural behavior and failure mode for prestressed concrete beams (Collins and Mitchell, 1997). A similar procedure was used to determine the behavior of steel-

concrete composite beams strengthened with unstressed or prestressed CFRP strips. This analysis is based on the cross-sectional geometry as well as the stress-strain behavior of the constituent materials.

The nominal flexural strength was evaluated using strain compatibility principles. It is important to note that since the ultimate strain of the FRP material will typically be reached well before the ultimate strain of the concrete, the equivalent rectangular stress block cannot be used. Thus, the moment-curvature analysis should be conducted using a constitutive model for the concrete to determine the compressive stresses at the limit state of the CFRP material. The flexural model assumes that plane sections remain plane when subjected to a bending moment. There is assumed to be a perfect bond between the CFRP material and the steel member. The bonded connection must be designed separately to ensure that this is true and that no premature debonding will occur. The flexural model satisfies conditions of strain compatibility and force equilibrium, and is based on the non-linear stress-strain behavior of the concrete and steel as well as the assumed linear behavior of the CFRP material. Constitutive models are selected to represent the behavior of the materials. Two different limit states may occur in the flexural model. The concrete at the extreme compression fiber may reach its ultimate strain or the CFRP strips may reach their ultimate strain in tension. The rupture may occur prior to steel yielding, which may be the case for high modulus CFRP materials, especially if they are prestressed, or the CFRP may rupture after yielding.

Analytical Procedure

The moment-curvature behavior for a given cross-section is determined based on a step-wise increase of the strain at the extreme fiber of the compression flange. The cross-section of the strengthened beam is broken down into segments corresponding to the concrete deck, the longitudinal steel reinforcement of the concrete deck, the flanges, and the web of the steel beam and the CFRP material at the bottom of the cross-section. The concrete stress may be described by a generalization of two expressions given by Popovics (1970) and found by Thorenfeldt *et al*. (1987) to be suitable for describing the compressive stress strain behavior for concretes with a range of strengths between 25 and 105 MPa. The reinforcing steel and the steel section were modeled using the modified Ramberg-Osgood function recommended by Mattock (1979). The parameters *A*, *B*, and *C* for each

material as well as the stiffness of the steel are provided in Table 6 as determined from the results of tension tests on the steel. Finally, the CFRP is modeled as a linear elastic material, accounting for any initial prestressing.

Calculations are continued until one of two limit states is reached; rupture of the FRP, or crushing of the concrete. Since both of these limit states are strain-controlled, and the process is based on incrementally increasing the strains, the ultimate strength and mode of failure are easily determined.

The load-deflection predictions using the proposed analytical procedure for beam HM-7.6-AB is shown in Figure 11. Similar predictions can be seen for the other beams in the experimental study in Schnerch (2005). Predictions were made for both the strengthened case and the unstrengthened case. The analytical model was able to closely match the load deflection behavior, failure mode, and ultimate strength for each of the beams tested. Table 5 lists the comparison between the predicted stiffness increases and rupture strengths for the test beams.

Parametric Study

For the ultimate strength of the steel-concrete composite beam after strengthening, the ultimate elongation of the FRP material may be even more important than the reinforcement ratio or the tensile modulus of the FRP material. Figure 12 shows the moment-curvature behavior of the baseline steel-concrete composite beam without the CFRP strengthening, as well as for the same beam reinforced with FRP strips with three different values of axial stiffness. Three different failure strains are indicated for each of these FRP strip types. The effect of the strengthening is to increase the stiffness of the beam before yielding, but even more so after steel yielding. It can also be seen that the strengthening changes the behavior of the system from one that is essentially elastic-plastic to one that is bilinear with a more significant second slope stiffness.

To determine the influence of the prestressing on the behavior of the system, a strengthening scheme with an axial FRP stiffness of 150 MN and an ultimate FRP elongation of 0.40 percent was considered. Figure 13 shows that the effect of increasing the amount of prestressing force, as a percentage of the ultimate strain of the CFRP material, is to shift the moment-curvature diagram such that more camber is possible, but with a lower ultimate

strength. The tradeoff in performance between the additional camber and the reduction in ultimate strength may be used beneficially in maintaining the full ductility of the beam, since after rupture of the CFRP, the behavior of the beam would revert to its unstrengthened state if the ultimate strength of the unstrengthened beam is not exceeded.

Design Procedure

Design guidelines for the use of high modulus FRP materials for strengthening steel bridges have been proposed (Schnerch et al. 2007). These guidelines consider the potential failure modes of FRP rupture, FRP debonding or compression failure of the concrete for steel-concrete composite beams. Other failure modes, such as shear failure of the web, must also be considered due to the increased loading of the beam. Since strengthening can increase the elastic stiffness of the beam, it follows that the steel strain in the tension flange is reduced compared to an unstrengthened beam at the same load level.

The allowable increase of live load for a strengthened steel-concrete composite beam should be selected to satisfy the three conditions shown in Figure 14. To ensure that the strengthened beam remains elastic under the effect of the increased live load, the total service load level, including the dead load, P_D, and the increased live load, P_L, should not exceed 60 percent of the calculated increased yield capacity, $P_{Y,S}$.

$$P_D + P_L \leq 0.6\, P_{Y,S} \qquad (1)$$

Secondly, to satisfy the ultimate strength requirements, the total factored load based on the appropriate dead load and live load factors, α_D and α_L, should not exceed the ultimate capacity of the strengthened beam $P_{U,S}$ after applying an appropriate strength reduction factor, ϕ.

$$\alpha_D P_D + \alpha_L P_L \leq P_{U,S} \qquad (2)$$

A strength reduction factor of 0.75 has been proposed for the brittle failure of CFRP materials, which is consistent with the reduction factor used by the American Institute of Steel Construction (AISC, 2001) for rupture type limit states. Finally, to ensure that the structure remains safe if the FRP system is damaged for some reason, the total load, including the dead load and increased live load should not exceed the residual capacity of the unstrengthened beam, $P_{N,\,US}$.

$$P_D + P_L \leq P_{N,US} \qquad (3)$$

The fatigue life of the strengthened member should also be checked according to the fatigue design provisions of the applicable design codes.

The flexural design is based only on the cross-section of the member, and a perfect bond is assumed to exist between the steel and FRP material. While this assumption is sufficient to predict the flexural behavior of the strengthened member up to the ultimate strength of the FRP material, a premature debonding failure will limit the capacity of the section. An analytical procedure has been developed for determining the bond stresses for a beam strengthened with externally bonded FRP materials, based on previous work completed in the UK (Cadei et al. 2004). The maximum principal stress in the adhesive is determined analytically based on the calculated shear and peel, or normal, stresses in the adhesive. This stress is compared to the stress that may be achieved from testing double-lap shear coupons using the same conditions of adhesive type, bondline thickness, surface preparation and substrate materials. Safety factors for bonded joints have been developed that take into account the method of adhesive application, the type of loading, environmental conditions, and the possibility for inspection of the joints (Institution of Structural Engineers, 1999).

Conclusions

Stiffness increases between 10 and 34 percent were found for the strengthened steel-concrete composite beams. Ultimate strength increases of up to 46 percent were possible for the strengthening configurations studied. The beam using the prestressed CFRP strips was shown to make economical use of the CFRP material in providing a

significant stiffness increase while maintaining the ductility of the original section. The assumption that plane strains remaining plane was shown to be valid. Additionally, the possibility of splicing finite lengths of CFRP strips was shown to be possible with an additional CFRP strip placed over the joint and wrapped with unidirectional sheets. A flexural model was developed based on strain compatibility and constitutive material properties that reasonably predicts the stiffness increase, ultimate strength increase, and failure mode of the member. This model was used to show that the use of high modulus strips is necessary to generate significant stiffness increases, whereas the axial stiffness and rupture strength of the CFRP strips are most important in determining the ultimate strength increase. Simple design guidelines are proposed based on this research.

Additional research in the strengthening of steel bridges should investigate the long-term performance of the bond between the steel and FRP. The use of pseudo-ductile FRP that are comprised of blends of different fiber materials may also be considered to reduce the possibility of sudden failure of the CFRP. The use of this technique may result in a concrete crushing failure mode and allow an appropriate safety factor to be used for this type of failure.

Acknowledgements

The authors would like to acknowledge the National Science Foundation (NSF) grant EEC-0225055, the NSF Industry/University Cooperative Research Center (I/UCRC) for the Repair of Buildings and Bridges with Composites (RB^{2}C) and Mitsubishi Chemical FP America.

Notation

The following symbols are used in this paper:

A = parameter in the Ramberg-Osgood function

B = parameter in the Ramberg-Osgood function

C = parameter in the Ramberg-Osgood function

P_D = dead load

P_L = live load

$P_{N,S}$ = nominal capacity of strengthened beam

$P_{N,US}$ = nominal capacity of unstrengthened beam

$P_{U,S}$ = ultimate capacity of strengthened beam

$P_{Y,S}$ = yield capacity of strengthened beam

$P_{Y,US}$ = yield capacity of unstrengthened beam

ϕ = strength reduction factor

References

Aglan, H., Wang Q.Y., and Kehoe, M. (2001). “Fatigue behavior of bonded composite repairs.” *Journal of Adhesion Science and Technology*, 15(3), 1621-1634.

Allan, R.C., Bird, J. and Clarke, J.D. (1988). “Use of adhesives in repair of cracks in ship structures.” *Materials Science and Technology*, 4(10), 853-859.

American Institute of Steel Construction (2001). *Manual of steel construction: load and resistance factor design,* 3rd ed.

Armstrong, K.B. (1983). “Carbon fibre fabric repairs to metal aircraft structures.” Engineering with Composites, *Proceedings of the Third Technology Conference,* SAMPE European Chapter, London, England, 8.1-8.12.

Cadei, J.M.C., T.J. Stratford, L.C. Hollaway, and W.G. Duckett (2004). *Strengthening metallic structures using externally bonded fibre-reinforced polymers.* CIRIA, Publication C595, London, UK, 2004, 234 p.

Clarke, J.L., ed. (1996). *Structural design of polymer composites: EUROCOMP design code and handbook*, E & FN Spon, London, UK, 751 p.

Collins, M.P. and Mitchell, D. (1997). *Prestressed Concrete Structures*, Response Publications, Canada, 766 p.

Colombi, P. and Poggi, C. (2006). "An experimental, analytical and numerical study of the static behavior of steel beams reinforced by pultruded CFRP strips." *Composites Part B: Engineering*, 37(1), 64-73.

Dawood, M. (2005). *Fundamental Behavior of Steel-Concrete Composite Beams Strengthened with High Modulus Carbon Fiber Reinforced Polymer (CFRP) Materials*, Master's Thesis, North Carolina State University, 212 p.

Edberg, W., Mertz, D. and Gillespie, J. Jr. (1996). "Rehabilitation of steel beams using composite materials." *Materials for the New Millennium, Proceedings of the ASCE Fourth Materials Engineering Conference*, Washington, D.C., 502-508.

El Damatty, A.A., Abushagur, M. and Youssef, M.A. (2003). "Experimental and analytical investigation of steel beams rehabilitated using GFRP sheets." *Steel and Composite Structures*, 3(6), 421-438.

Galbraith, D.N. and Barnes, F. (1995). "Beryl Bravo – blast walls conversion: Development and testing of steel/carbon fibre composite." *Proceedings of the 5th International Offshore and Polar Engineering Conference*, The Hague, The Netherlands, 229-236.

Hollaway, L.C. and Cadei, J. (2002). "Progress in the technique of upgrading metallic structures with advanced polymer composites." *Progress in Structural Engineering Materials*, 4(2), 131-148.

Institution of Structural Engineers (1999). *A Guide to the Structural Use of Adhesives.* The institution of Structural Engineers, London, UK, 51 p.

Lee, Y.S., Wipf, T.J., Phares, B.M. and Klaiber, F.W. (2005). "Evaluation of a steel bridge girder strengthened with CFRP post-tension bars." *Transportation Research Record*, n. 1928, 233-244.

Liu, X., Silva, P.F., and Nanni, A. (2001). "Rehabilitation of steel bridge members with FRP composite materials." *Proceedings of the International Conference on Composites in Construction*, J. Figueiras, L. Juvandes and R. Furia, eds., Porto, Portugal, 613-617.

Luke, S. (2001). "The use of carbon fibre plates for the strengthening of two metallic bridges of an historic nature in the UK." *International Conference on FRP Composites in Civil Engineering*, J. G. Teng, ed., Hong Kong, China, v. 2, 975-983.

Mattock, A.H. (1979). "Flexural strength of prestressed concrete sections by programmable calculator." *PCI Journal*, 24(1), 32-54.

Miller, T.C., Chajes, M.J., Mertz, D.R. and Hastings, J.N. (2001). "Strengthening of a steel bridge girder using CFRP plates." *ASCE Journal of Bridge Engineering*, 6(6), 514-522.

Phares, B.M., Wipf, T.J., Klaiber, F.W., Abu-Hawash, A. and Lee, Y.S. (2003). "Strengthening of steel girder bridges using FRP." *Proceedings of the 2003 Mid-Continent Transportation Research Symposium*, Ames, Iowa.

Popovics, S. (1970). "A review of stress-strain relationships for concrete." *ACI Journal*, 67(3), 243-248.

Schnerch, D.A. (2005). *Strengthening of Steel Structures with High Modulus Carbon Fiber Reinforced Polymer (CFRP) Materials*, Ph.D. Dissertation, North Carolina State University, 265 p.

Schnerch, D., Dawood, M., Rizkalla, S. and Sumner, E. (2007). “Proposed design guidelines for strengthening of steel bridges with FRP materials.” *Construction and Building Materials,* Accepted for publication.

Sen, R., Liby, L., and Mullins, G. (2001). “Strengthening steel bridge sections using CFRP laminates.” *Composites Part B: Engineering*, 32(4), 309-322.

Tavakkolizadeh, M. and Saadatmanesh, H. (2003). “Strengthening of steel-concrete composite girders using carbon fiber reinforced polymer sheets.” *Journal of Structural Engineering*, ASCE, 129(1), 30-40.

Thorenfeldt, E., Tomaszewicz, A. and Jensen, J.J. (1987). “Mechanical properties of high-strength concrete and application in design.” *Proceedings of the Symposium Utilization of High Strength Concrete and Application in Design*, Stavanger, Norway, Tapir, Trondheim, 149-159.

Tables

Table 1. CFRP strip properties for two types of strips used in the experimental program

Property	DC-I	THM 450
Fiber volume fraction (%)	55 %	70 %
Tensile strength (MPa)	1224	1534
Tensile modulus (GPa)	229	457
Ultimate elongation (%)	0.508	0.332
Strip thickness (mm)	3.2	2.9 or 4.0

Table 2. Material Properties for Steel-Concrete Composite Beams

Property	IM-4.5-AB & HM-3.8-PS	HM-7.6-AB
Concrete strength, f'_c (MPa)	43	37
Steel yield (flanges) f_y (MPa)	378	369
Steel yield (webs) f_y (MPa)	407	408
Steel yield (rebar) f_y (MPa)	463	436

Table 3. Stiffness comparison for strengthened beams at 60 percent yield of the tension flange

	Unstrengthened		Strengthened	
Beam	Total load (kN)	Net midspan deflection (mm)	Total load (kN)	Net midspan deflection (mm)
IM-4.5-AB	150	15.8	173	16.3
HM-3.8-PS	151	15.2	184	14.1[a]
HM-7.6-AB	152	15.0	226	16.4

[a] Accounting for the beneficial effect of camber

Table 4. Properties at rupture and concrete crushing for strengthened steel-concrete composite beams

	At CFRP rupture		At concrete crushing	
Beam	Total load (kN)	Net midspan deflection (mm)	Total load (kN)	Net midspan deflection (mm)
IM-4.5-AB	418	54.2	358	141.5
HM-3.8-PS	343	33.1[a]	346	124.4[a]
HM-7.6-AB	491	44.3	338	114.6

[a] Accounting for the beneficial effect of camber

Table 5. Comparison of predicted and experimental results for strengthened steel-concrete composite beams

	Stiffness increase		Strength at rupture	
Beam	Predicted	Experimental	Predicted	Experimental
IM-4.5-AB	16 %	10 %	442 kN	418 kN
HM-3.8-PS	31 %	31 %	381 kN	343 kN
HM-7.6-AB	40 %	36 %	517 kN	491 kN

Table 6. Ramberg-Osgood Parameters used in Analysis

Parameter	Flange	Web	Reinforcing
A	0.0	0.0	0.1
B	572.0	530.4	454.8
C	20.0	20.0	3.4

Figure Captions

Figure 1. Cross-section dimensions of steel-concrete composite beams

Figure 2. Strengthening configuration of steel-concrete composite beams

Figure 3. Configuration of taper at end of strip

Figure 4. Fixed piece of prestressing fixture at jacking end

Figure 5. Configuration of fixture to apply jacking force at jacking end

Figure 6. Typical loading configuration of steel-concrete composite beams

Figure 7. Load-Deflection Behavior and Strain Profiles of Beam IM-4.5-AB

Figure 8. Load-Deflection Behavior and Strain Profiles of Beam HM-3.8-PS

Figure 9. Load-Deflection Behavior and Strain Profiles of Beam HM-7.6-AB

Figure 10. Rupture of the CFRP Strips of Strengthened Beam HM-7.6-AB

Figure 11. Comparison of Load-Deflection Behavior for Steel-Concrete Composite Beam HM-7.6-AB

Figure 12. Effect of Axial Stiffness and Ultimate Elongation

Figure 13. Effect of Prestressing Level on Behavior of Typical Strengthened Beam

Figure 14. Calculation of Allowable Live Load for Typical Strengthened Beam

Figures

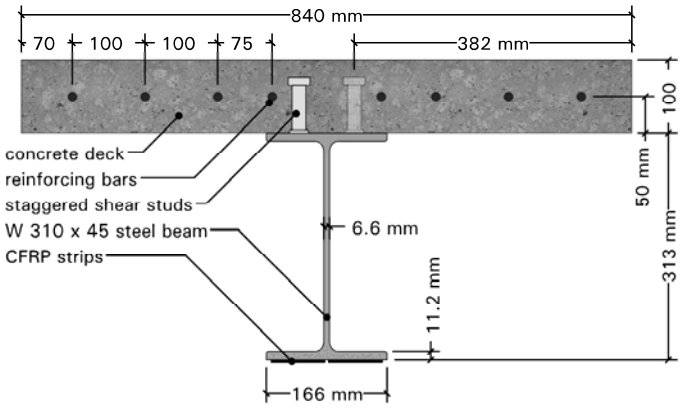

Figure 1. Cross-section dimensions of steel-concrete composite beams

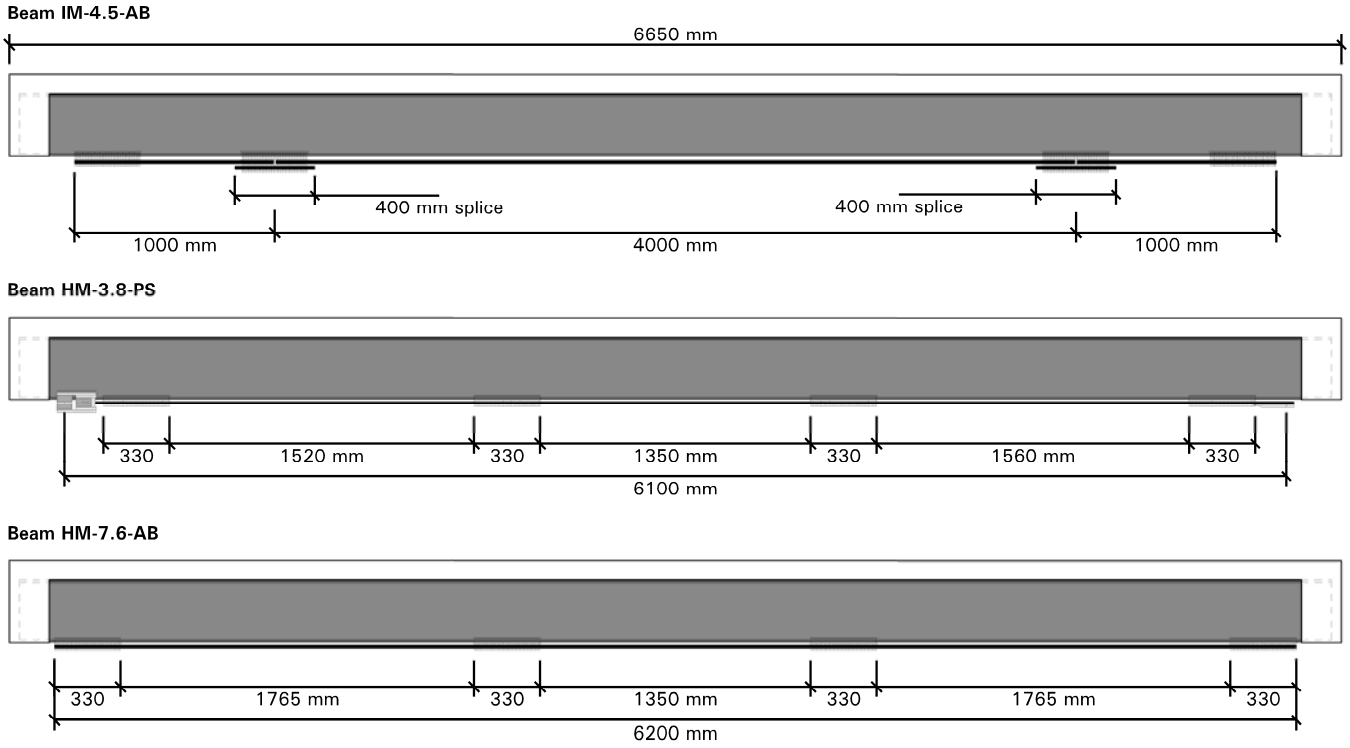

Figure 2. Strengthening configuration of steel-concrete composite beams

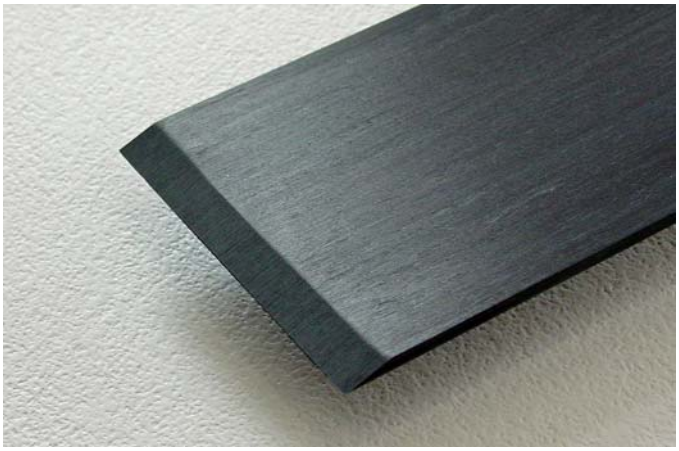

Figure 3. Configuration of taper at end of strip

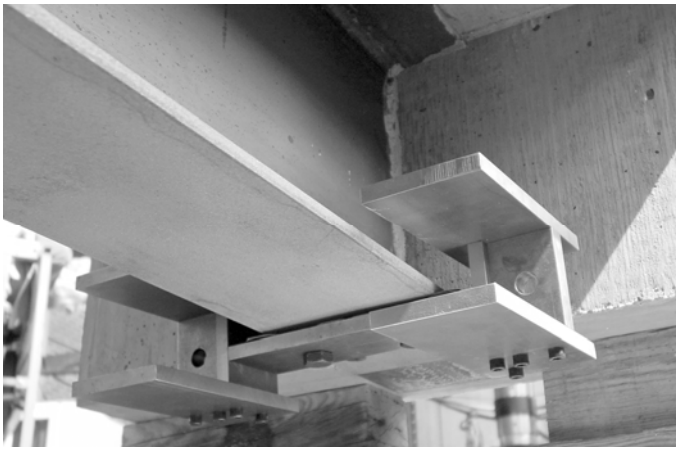

Figure 4. Fixed piece of prestressing fixture at jacking end

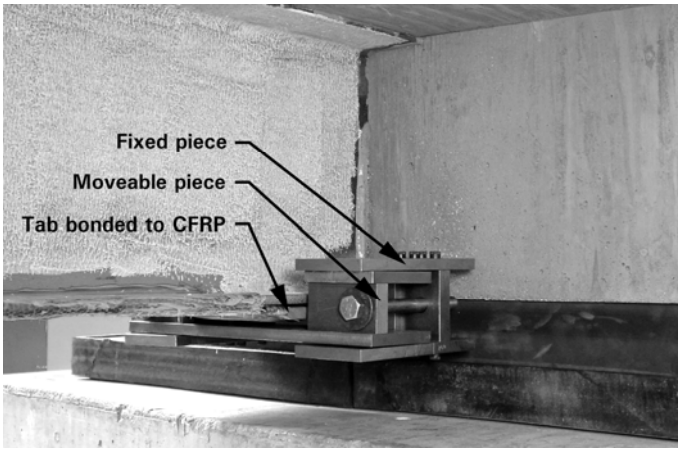

Figure 5. Configuration of fixture to apply jacking force at jacking end

Figure 6. Typical loading configuration of steel-concrete composite beams

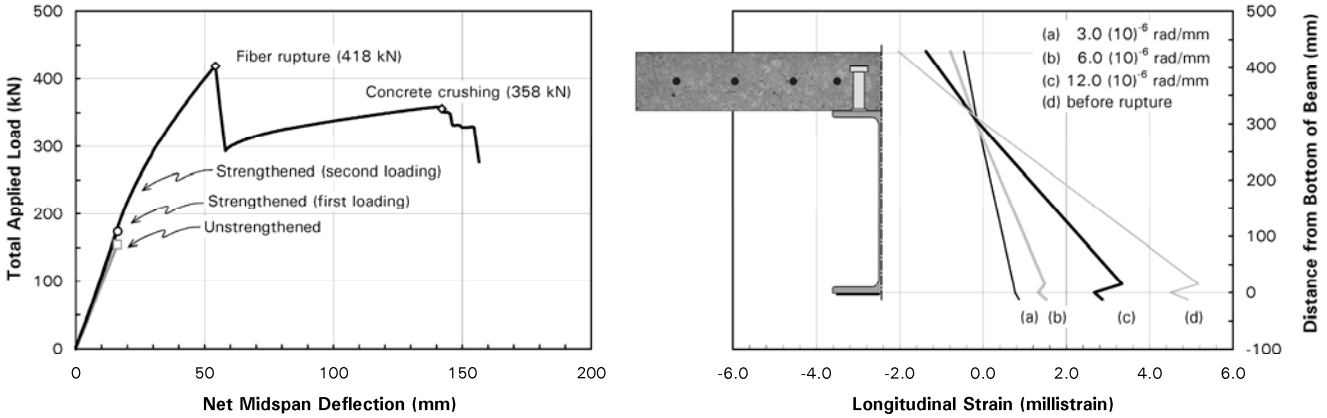

Figure 7. Load-Deflection Behavior and Strain Profiles of Beam IM-4.5-AB

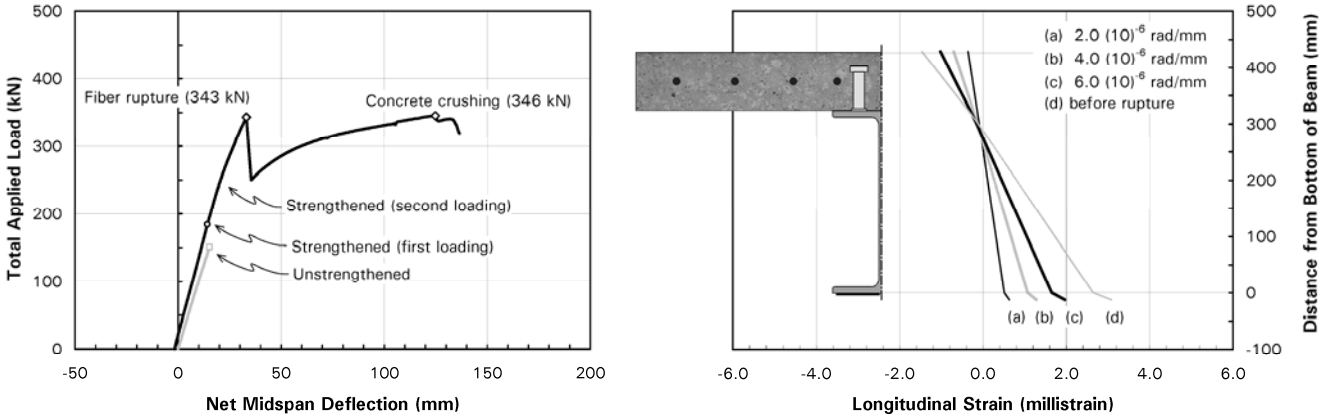

Figure 8. Load-Deflection Behavior and Strain Profiles of Beam HM-3.8-PS

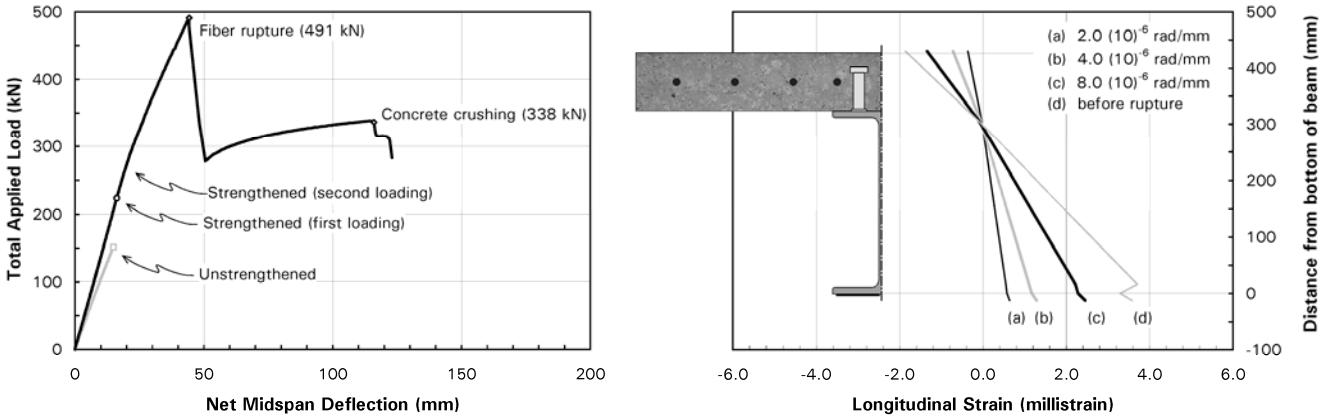

Figure 9. Load-Deflection Behavior and Strain Profiles of Beam HM-7.6-AB

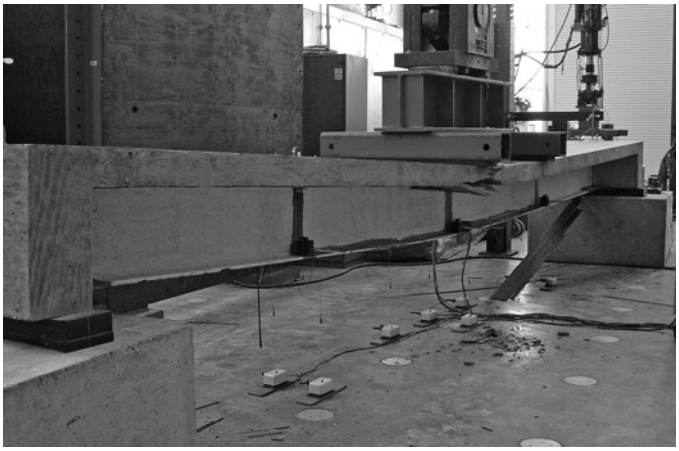

Figure 10. Rupture of the CFRP Strips of Strengthened Beam HM-7.6-AB

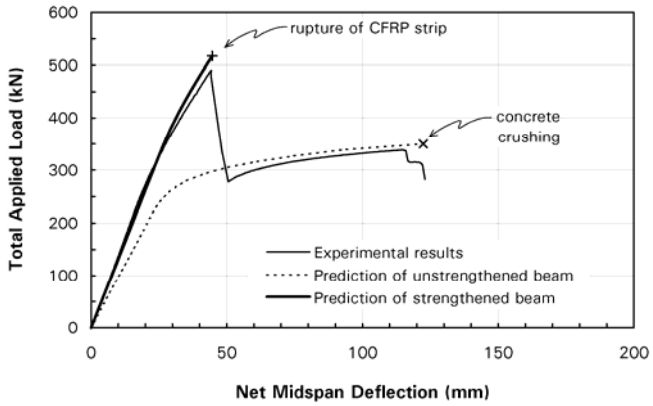

Figure 11. Comparison of Load-Deflection Behavior for Steel-Concrete Composite Beam HM-7.6-AB

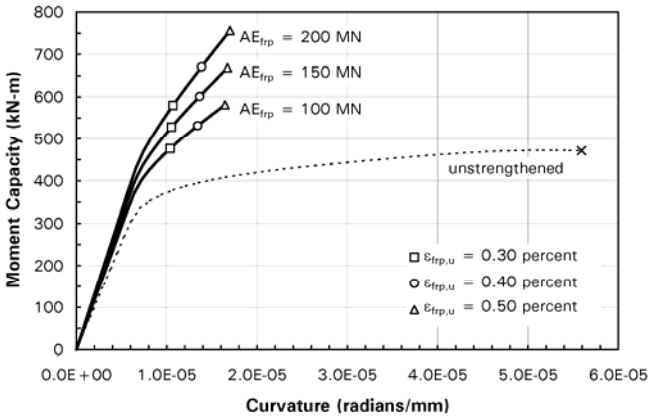

Figure 12. Effect of Axial Stiffness and Ultimate Elongation

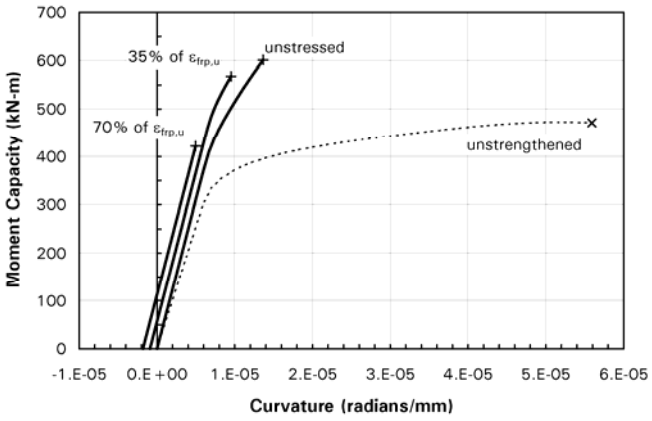

Figure 13. Effect of Prestressing Level on Behavior of Typical Strengthened Beam

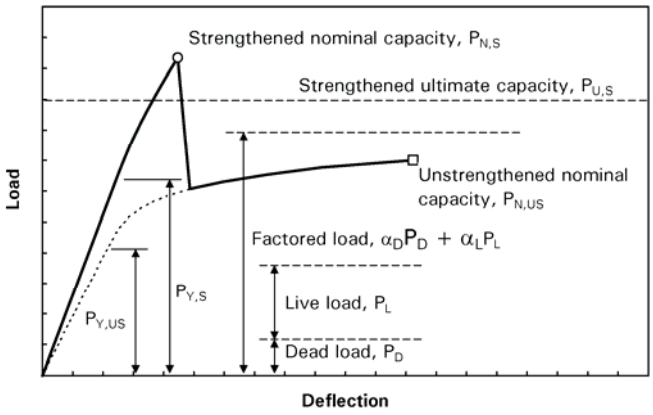

Figure 14. Calculation of Allowable Live Load for Typical Strengthened Beam